JAST, Vol. 7, No. 2, pp 139–150


JAST Journal of Aerospace Science and Technology

Research Note

# Improvement in Differential GPS Accuracy Using Kalman Filter

M. R. Mosavi[1], A. Nakhaei[2] and Sh. Bagherinia[3]

*Global Positioning System (GPS) has proven to be an accurate positioning sensor. However, it is associated with several sources of error such as ionosphere and troposphere effects, satellite time errors, errors of orbit data, receiver's errors, and errors resulting from multi-path effect which reduce the accuracy of low-cost GPS receivers. These sources of error also limit the use of single-frequency GPS receivers due to their less accurate data. Therefore, it's important to reduce the effect of errors on GPS systems. In order to cope with these errors and enhance GPS system's accuracy, Differential GPS (DGPS) method can be used. The problem with this method is slow updating process of differential corrections. In this paper, three algorithms based on Kalman Filtering (KF) are proposed to predict real-time corrections of DGPS systems. The efficiency of the proposed algorithms is verified on the basis of actual data. The experimental results obtained in field tests gaurantee the high potential of these methods to get accurate positioning data. The results show that KF with variable transition matrix is better than other methods; so it's possible to reduce the Root Mean Square (RMS) of positioning errors in low-cost GPS receivers to less than one meter.*

## INTRODUCTION

GPS is a navigation and positioning satellite system which is comprised of a network of at least 24 satellites. The satellites are continuously in contact with specially designated ground-based stations and their position in orbital constellation is always known. Using messages received from a minimum of four satellites, a GPS receiver is able to determine user's absolute position anywhere on the earth's surface. Doing various measurements, the receiver calculates time, velocity, distance between user and destination, (longitude, latitude, and altitude), time of sunrise and sunset, local time, *etc.* which are finally shown to the user [1]. During different phases of signals transmission, receipt, and their analysis in GPS systems, various errors will affect the whole procedure [2].

1. *(Corresponding Author), Associate Professor, Dept. of Electrical Eng., Iran University of Science and Technology, Tehran, Iran, Email: M_Mosavi@iust.ac.ir.*
2. *M.Sc. Student, Dept. of Electrical Eng., Iran Univ. of Sci. and Tech., Tehran, Iran.*
3. *B.Sc. Student, Dept. of Electrical Eng., Iran Univ. of Sci. and Tech., Tehran, Iran.*

The purpose of this paper is to present three algorithms based on Kalman Filter (KF) in order to predict Differential GPS (DGPS) corrections. This paper is organized as follows. At first, the sources of error in GPS systems and DGPS, the process of design and implementation of KF-based estimators will be discussed. Then, the adopted data collection method and the experimental test analyses, carried out on the collected actual data, are reported. Conclusions are presented in the last section.

## SOURCES OF ERROR IN GPS

Categorization of the significant sources of error in GPS systems is usually based on their type and main characteristics as well as the researcher's point of view. Therefore, there would be various categorizations due to the constant sources of error and their different level of importance for the researchers. Generally, the sources of error are categorized into three main groups as follows [3]:

a. Errors related to satellites (caused by satellite clock and geometry),

b. Propagation errors (caused by ionosphere and troposphere effects),

c. Errors related to the receiver equipment (caused by the applied technology in GPS receivers).

In the following section, these sources of errors will be discussed further.

### Satellite Clock Errors

In order to control the different functions carried out by a satellite, a number of clocks are utilized. One of the functions, under the control of the satellite clocks, is generating GPS satellite signals. To increase the reliability and possibility of substitution, in each satellite, two rubidium and two cesium clocks are used. These clocks are corrected and adjusted every day by the GPS control segment. It should be mentioned that the errors caused by these clocks, working for 24 hours, is equal to 17 [nsec] or 5 [m] in length [4].

### Errors in Satellite's Astrological Data

GPS signals contain a Pseudo Random Code (PRC), a segment for satellite's orbital position information (ephemeric), and another segment for calendar data (almanac). The PRC contains satellite's identification information and determines which satellite is transmitting the signal. Satellite position errors occur because the above-mentioned information gets updated continuously. In order to prevent these errors, they should get corrected during the defined time intervals. In other words, there are some differences between the actual satellite position and their predicted position. Ideally, satellites are positioned on very precise orbits in the space. However, in reality, there would be some changes in ephemeris data.

### Ionospheric Layer Errors

While we study sources of error in GPS systems, we are always faced with a concept called ionosphere effect. Ionosphere is a shell of electrons and electrically charged atoms and molecules that surrounds the earth, stretching from a height of about 50 kilometers to more than 1,000 kilometers. In fact, the energy from the sun's radiations impinges on the atoms and molecules in the upper atmosphere, breaks some of the bonds that hold electrons to atoms or ionizes atoms and molecules. The result of ionization is a large number of free, negatively-charged, electrons and positively-charged atoms and molecules called ions. Therefore, this layer of atmosphere is called ionosphere. The ionization degree varies in different heights of ionosphere layer. Free electrons in ionosphere layer can cause errors in GPS signals in proportion to the user's position. These errors usually cause two primary effects on a GPS signal. The first causes errors with refracting and diffracting the signal's path. The second causes delays on the signal which is sent from the satellite to the receiver [5].

### Multi-Path Effect Errors

The multi-path effect happens when GPS signals sent by a satellite are received by a receiver in various ways and following different paths because they are reflected by surrounding terrain: buildings, canyon walls, hard ground, etc. As a result, the signals are delayed and it takes them more time to reach the receiver than the direct signals.

### GPS Receiver Errors

The GPS receiver specific errors are mainly classified into receiver clock errors, the noise affecting the receiver, satellite selection algorithm errors, and errors caused by calculation algorithms.

### Selective Availability

Selective Availability (SA) is a deliberate error which reduces the potential for GPS signal to be used in hostilities toward the USA and its allies. The SA's most important feature is its being independent from different satellites. At first, the amount of error affecting receivers was set to 500 meters. Afterwards, in 1983, this amount was reduced to almost 100 meters and finally in 1990, this source of error was officially applied. The SA caused position determination error to decrease by 100 meters horizontally and reduced height measurement accuracy by 156 meters with the possibility of 95 percent. In fact, from the civil user's point of view, errors resulted from the SA is like a sinus function which varies over time and it affects measuring pseudo distances with the Root Mean Square (RMS) equal to almost 25 meters [6].

Table 1 illustrates the average amount of typical GPS satellite errors in meters.

## DGPS METHOD

In order to prevent errors and increase accuracy, the reliable DGPS method can be utilized. In this technique, a second receiver has to be set up on a precisely known location. This receiver uses transmitted signals from the satellites to calculate its location and measures the difference between the satellite indicated location and the already known fixed location. As a result, the system errors and inaccuracies will be detected and then the required information for correcting the errors will be calculated and broadcast to the other

**Table 1.** The average of typical GPS satellite system errors in meters [7].

| Error Source | Value |
|---|---|
| Receiver noise | 0.4 |
| Troposphere | 0.5 |
| Multi-path | 0.6 |
| Satellite clock | 1.5 |
| Satellite orbit | 2.5 |
| Ionosphere | 5 |
| SA | 30 |

GPS receivers located in the area. The receivers, based on the correction signal, apply the needed corrections to their calculated data. This method can improve static positioning (for example land surveying) up to some centimeters as well as kinetic positioning up to some meters [8]. It is obvious that, in real-time DGPS systems, in addition to a reference receiver-transmitter system, some other special receivers are needed. In non real-time systems (*e.g.* land surveying), information transmitted by satellites is collected and stored simultaneously in two fixed and known positions. Subsequently, this information is transferred to a central computer system to be processed by special software and finally the precise position data will be obtained. The main problem in DGPS method is the slow process of updating differential corrections. In order to predict real-time differential GPS corrections, three algorithms based on KF are proposed in this paper.

## KALMAN FILTER

KF is an efficient estimator which exploits state space principle and system error modeling, resulting in optimum prediction of system state. One of the KF's important features is its recursive calculation which stores the last step of calculations and, hence, uses small capacity of memory and updates the previous calculations when new information is received [9].

### Second Order KF with Constant Transition Matrix

In this section, the general discrete KF is formulated which is comprised of two phases, namely, estimation and correction. The process is governed by two equations, a stochastic difference equation which estimates the process and a measurement equation which illustrates the measurement process as follows [10]:

$$S[n] = \phi S[n-1] + W[n] \tag{1}$$

$$X[n] = HS[n] + \gamma[n] \tag{2}$$

In the above equations, $S[n]$ and $S[n-1]$ are $2 \times 1$ matrixes which represent the state of system at $n$ and $n-1$ times, respectively. $\phi$ is a known $2 \times 2$ constant matrix as well as $H$ which is a known $1 \times 2$ constant matrix. $X[n]$ is $1 \times 1$ measurement vector, $W[n]$ is a $2 \times 1$ vector which demonstrates system modeling noise, and $\gamma[n]$ is a $1 \times 1$ vector representing measurement noise. $R$ and $Q$ are representing covariance matrixes of processes $\gamma[n]$ and $W[n]$ . The processes $\gamma[n]$ and $W[n]$ are independent, zero mean Gaussian proportional to $\sigma_\omega^2$ and $\sigma_y^2$ variances. The constant matrix $\phi$ (state transition matrix) is defined as follows:

$$\phi = \begin{bmatrix} 0 & 1 \\ \alpha_2 & \alpha_1 \end{bmatrix} \tag{3}$$

$\alpha_1$, $\alpha_2$ and also $\sigma_\omega^2$ coefficients are estimated using autocorrelation equations as described below:

$$\alpha_1 = \frac{R_{SS}(0)\, R_{SS}(1) - R_{SS}(1)\, R_{SS}(2)}{R_{SS}^2(0) \; - R_{SS}^2(1)} \tag{4}$$

$$\alpha_2 = \frac{-R_{SS}^2(1) \; + R_{SS}(0)\, R_{SS}(2)}{R_{SS}^2(0) \; - R_{SS}^2(1)} \tag{5}$$

$$\sigma_\omega^2 = R_{SS}(0) - \alpha_1 R_{SS}(1) - \alpha_2 R_{SS}(2) \tag{6}$$

which:

$$\hat{R}_{SS}[k] = E\{S[i]S[i+k]\} \;\; ; \quad k = 0,\, 1,\, 2 \tag{7}$$

The brief description of second-order KF algorithm with constant transition matrix is as follows [11]:

**Step 1:** Initialize KF parameters

$$R = [\sigma_\omega^2] \tag{8}$$

$$Q = \begin{bmatrix} 0 & 0 \\ 0 & \sigma_\omega^2 \end{bmatrix} \tag{9}$$

$$P_0 = \begin{bmatrix} 1 & 0 \\ 0 & 1 \end{bmatrix} \tag{10}$$

$$S_0 = \begin{bmatrix} 0 \\ 0 \end{bmatrix} \tag{11}$$

$$H = [0 \quad 1] \tag{12}$$

**Step 2:** Generate the state transition matrix $\phi$ using (3), (4), and (5) equations.

**Step 3:** Compute the Kalman gain

$$K[n] = P^-[n]H^T(H[n]P^-[n]H^T[n] + R[n])^{-1} \tag{13}$$

**Step 4:** Update the estimation process

$$\hat{S}[n] = \hat{S}^-[n] + K[n](X[n] - H[n]\hat{S}^-[n]) \tag{14}$$

**Step 5:** Update the error covariance

$$P[n] = (I - K[n]H[n])P^-[n] \tag{15}$$

Until this step, the correction phase is accomplished. From the next step, the estimation or updating phase will be executed.

**Step 6:** Project the state ahead

$$\hat{S}^{-}[n+1] = \phi[n]\hat{S}[n] \quad (16)$$

**Step 7:** Project the error covariance ahead

$$P^{-}[n+1] = \phi[n]P[n]\phi^{T}[n] + Q[n] \quad (17)$$

It should be mentioned that under conditions where $H$, $\phi$, $R$, and $Q$ are constant, both the estimation error covariance and the Kalman gain will stabilize quickly and then remain constant. By pre-computing these parameters and using them in Kalman algorithm, there would be no need for updating them in the subsequent steps.

### KF with Gauss-Markov Process

A stationary Gauss-Markov process is a Gauss-Markov process which has an exponential autocorrelation factor. The autocorrelation and spectral functions for this process are illustrated below [12]:

$$R_x(\tau) = \sigma^2 e^{-\beta|\tau|} \quad (18)$$

$$S_x(j\omega) = \frac{2\sigma^2\beta}{\omega^2 + \beta^2} \quad (19)$$

In this process, the mean square (variance) and time constant parameters are $\sigma^2$ and $1/\beta$, respectively.

The researches have shown that utilizing second-order Gauss-Markov process with Power Spectral Density (PSD) function can improve measurement accuracy [1].

$$PSD = S(\omega) = \frac{C}{\omega^4 + \omega_0^4} \quad \left[\frac{m^2}{Rad.Sec^{-1}}\right] \quad (20)$$

In equation (20), $C$ demonstrates a constant which is defined by a range of variations. When SA mode is turned on, $\omega_0$ is almost equal to 0.012 $Rad.Sec^{-1}$. Based on the fact that the RMS of SA error is defined equal to 30 meters, the parameter $C$ can be calculated using the equation below:

$$\frac{1}{2\pi j}\int_{-j\infty}^{+j\infty} \left(\frac{C}{S^4 + \omega_0^4}\right)ds = \frac{C}{(2\sqrt{2})\omega_0^3} = (30m)^2 \quad (21)$$

The above equation yields $C = 0.0043987m^2(Rad.Sec^{-1})^3$.

The continuous state model of this process is calculated using the equations below [1]:

$$\begin{bmatrix} \dot{x}_1 \\ \dot{x}_2 \end{bmatrix} = \begin{bmatrix} 0 & 1 \\ -\omega_0^2 & -\sqrt{2}\omega_0 \end{bmatrix} \begin{bmatrix} x_1 \\ x_2 \end{bmatrix} + \begin{bmatrix} 0 \\ \sqrt{C} \end{bmatrix} u(t) \quad (22)$$

Another equivalent formulation for the above matrix-based equation is:

$$\dot{X} = FX + GU \quad (23)$$

Because the Eq. (23) is a continuous time process, using a sampled time $\Delta t$ and Van Loan's proposed method, the matrixes $\phi_n$ and $Q_n$ can be calculated as follows:

$$A = \begin{bmatrix} -F\Delta t & GWG^T\Delta t \\ 0 & F^T\Delta t \end{bmatrix} \quad (24)$$

$$B = e^A = \begin{bmatrix} \cdots & \phi_n^{-1}Q_n \\ 0 & \phi_n^T \end{bmatrix} \quad (25)$$

Transposing the right below quarter of the above matrix results in $\phi_n$, and the right above quarter of it helps to calculate the $Q_n$ matrix.

### Second-Order KF with Variable Transition Matrix

In this method, the state vector transition matrix $\phi_n$ is computed using the Auto-Regressive (AR) time variant model. This model is one of the famous models which is applicable in random discrete time processes. The AR model in time domain is described as follows [13]:

$$y(n) = -\sum_{i=1}^{i=p} \alpha_i(n)y(n-i) + e(n) \quad (26)$$

where $y(n-i)$ demonstrates the outputs of the model, and $e(n)$ describes noise of the system at time $n$. $\alpha_i$ is a set of parameters which describe the model and the default value is always $\alpha_0 = 1$.

To identify the system, first the parameters $\alpha_i$ should be calculated in a way that summation of square errors gets the minimum value. Therefore, this method is called Least Squares (LS).

In case of applying the above-mentioned method on the AR model, the parameter matrixes are calculated as below [13]:

$$\theta = \left[F^T(N)F(N)\right]^{-1} F^T(N)Y(N) \quad (27)$$

where the matrix $\theta$ represents factors of AR model and matrices $Y(N)$ and $F(N)$ are calculated as follows:

$$Y(N) = [y(n) \quad y(n+1) \quad \cdots \quad y(N)]^T \quad (28)$$

$$F(N) = \left[f^T(n) \quad f^T(n+1) \quad \cdots \quad f^T(N)\right]^T \quad (29)$$

where the $f^T(n)$ matrix is defined as it is shown below:

$$f^T(n) = [y(n-1) \quad y(n-2) \quad \cdots \quad y(n-p)] \quad (30)$$

It should be mentioned that, by defining the matrix of factors, the value of function $y(n)$ at the time $n$ can be computed as follows:

$$y(n) = -\sum_{i=1}^{i=p} a_{p-i+1}(n)y(n-i) \tag{31}$$

In order to generate state space, some AR differential equations should be used as the following sequence of equations shows:

$$\begin{aligned} x_1(n) &= y(n-p) \\ x_2(n) &= x_1(n+1) = y(n-p+1) \\ x_3(n) &= x_2(n+1) = y(n-p+2) \\ &\vdots \\ x_{p+1}(n) &= x_p(n+1) = y(n) \end{aligned} \tag{32}$$

or

$$\begin{aligned} x_1(n+1) &= x_2(n) \\ x_2(n+1) &= x_3(n) \\ &\vdots \\ x_p(n+1) &= -a_p x_p(n) - a_{p-1}x_{p-1}(n) \\ &\quad - \cdots - a_1 x_1(n) \end{aligned} \tag{33}$$

The equivalent matrix-based formulation of the Eq. (33) can be:

$$\begin{bmatrix} x_1 \\ x_2 \\ \vdots \\ x_p \end{bmatrix}_{n+1} = \begin{bmatrix} 0 & 1 & 0 & \cdots & 0 \\ 0 & 0 & 1 & \cdots & 0 \\ \vdots & \vdots & \vdots & \vdots & \vdots \\ -a_1 & -a_2 & -a_3 & \cdots & -a_p \end{bmatrix} \begin{bmatrix} x_1 \\ x_2 \\ \vdots \\ x_p \end{bmatrix}_n \tag{34}$$

in which the transition matrix $\phi_n$ is resulted:

$$\phi_n = \begin{bmatrix} 0 & 1 & 0 & \cdots & 0 \\ 0 & 0 & 1 & \cdots & 0 \\ \vdots & \vdots & \vdots & \vdots & \vdots \\ -a_1 & -a_2 & -a_3 & \cdots & -a_p \end{bmatrix} \tag{35}$$

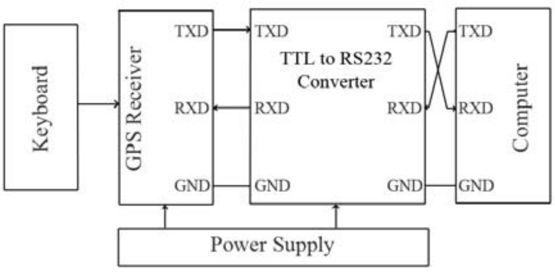


**Figure 1.** The block diagram of data collection hardware.

## DATA COLLECTION

In order to assess the efficiency and functionality of the methods proposed so far in this paper, collecting actual data seems to be absolutely essential. The data collection process has been accomplished on the building of Computer Control and Fuzzy Logic Research Lab in the Iran University of Science and Technology. Figure 1 depicts the block diagram of the hardware used in data collection process.

According to the hardware shown in Figure 1, the serial GPS receiver data are passed through TTL-RS232 converter to change their levels from TTL to RS232 standard and become ready to be connected to the computer. It should be noted that the keyboard on this hardware board is used for the purpose of setting GPS receiver's programmable parameters such as the output protocol of receiver's serial ports (NMEA or Binary) and data transmission rate (4600 or 9600 bit/s).

The technical features of the GPS receiver used in data collection process are [14]:

- 5 parallel channels,
- Capable of tracking and measuring up to 9 satellites,
- Supporting NMEA-0183 protocols with NMEA approved and developed messages,
- Capability of receiving differential RTCM SC-104 messages in order to increase positioning accuracy in differential mode,
- Capability of decreasing SA effect in static positioning,
- Measuring velocity up to 950 m/sec (3420 km/sec) and acceleration 4g,
- Working with active and inactive antennas,
- Maximum position measuring accuracy in SPS mode,
- Maximum operating flexibility with user's commands,
- Capability of satellite selection and limiting view angle of satellites,
- Horizontal accuracy equal to 100 meters and vertical accuracy equal to 188 meters,
- Information update rate 1 second,
- TMP or 1PPS output with accuracy of ± MSec,
- Serial output protocol: binary or NMEA with speed rate of 4800 or 9600 bit per second,
- RF input impedance 50 ohms with the acceptable input power -163 dBW to -130 dBW.

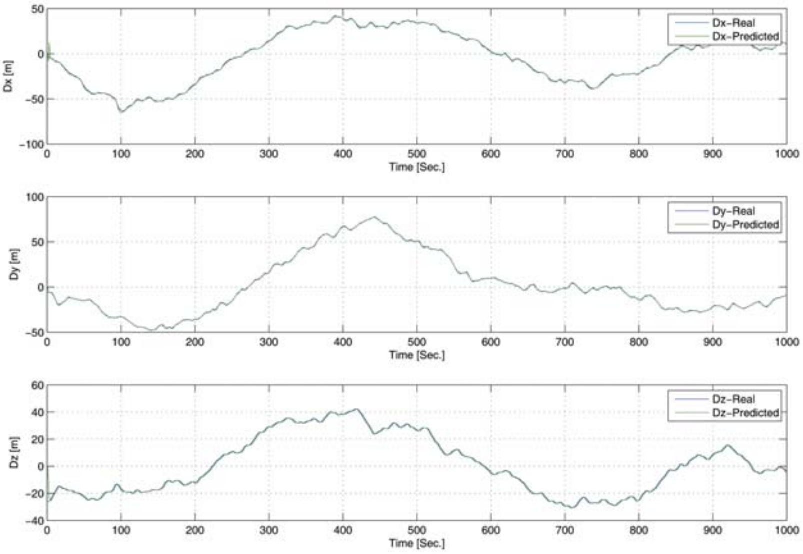


**Figure 2.** The results of 1000 prediction for component positions using KF with constant transition matrix (SA on).

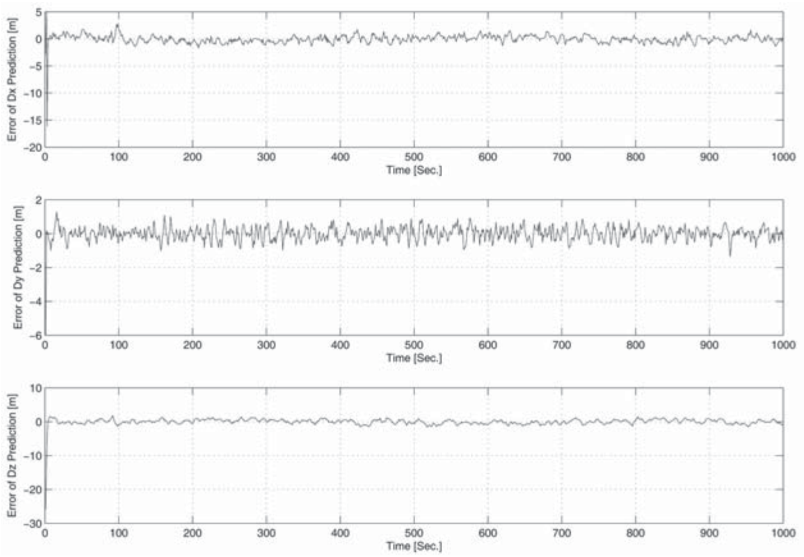


**Figure 3.** The results of 1000 prediction error for component positions using KF with constant transition matrix (SA on).

## EXPERIMENTAL RESULTS

Figures 2 to 5 represent the real, predicted and prediction error values of the component position errors for 1000 experimental data sets using KF with constant transition matrix in SA error turned on and turned off states.

Tables 2 and 3 depict the statistical features of estimation errors for the tests which have been accomplished on experimental data.

According to the results illustrated in Tables 2 and 3, it's noticeable that the RMS errors in estimation error of component positions using KF with constant transition matrix in SA on and off modes reduced to less than 1.5 and 0.9 meters, respectively. The results from the tests carried out on real data show that the functionality of KF in estimating components of

**Table 2.** Minimum, maximum, average, and RMS of errors in predicting 1000 experimental data sets using KF with constant transition matrix (SA on).

| Parameters | x | y | z |
|---|---|---|---|
| Max | 4.9861 | 1.2761 | 1.8113 |
| Min | -16.1242 | -5.9845 | -25.9376 |
| Average | 0.0327 | 0.0045 | 0.0122 |
| RMS | 0.8281 | 0.4268 | 1.0953 |
| **Total RMS** | **1.4380** | | |

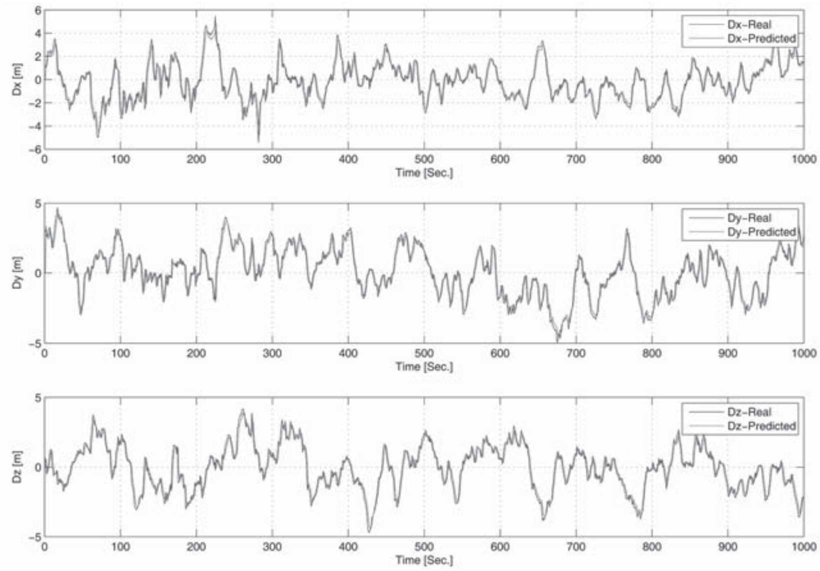


**Figure 4.** The results of 1000 prediction for component positions using KF with constant transition matrix (SA off).

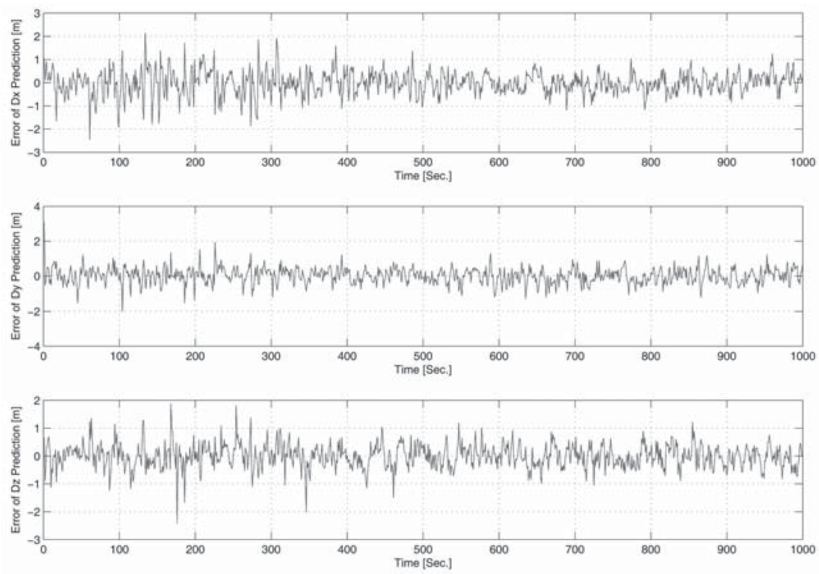


**Figure 5.** The results of 1000 prediction error for component positions using KF with constant transition matrix (SA off).

position errors is independent of the effect of SA errors which is one of the advantages of KF.

Figures 6 to 9 illustrate the real, predicted and prediction error values of the component position errors for 1000 experimental data sets using KF with Gauss-Markov modeling in SA error turned on and turned off modes.

**Table 3.** Minimum, maximum, average, and RMS of errors in predicting 1000 experimental data sets using KF with constant transition matrix (SA off).

| Parameters | x | y | z |
|---|---|---|---|
| Max | 2.1349 | 3.0893 | 1.8759 |
| Min | -2.4570 | -2.0089 | -2.4190 |
| Average | 0.0128 | -0.0084 | 0.0058 |
| RMS | 0.5181 | 0.4550 | 0.4269 |
| **Total RMS** | **0.8108** | | |

Tables 4 and 5 show the statistical characteristics of prediction errors for the experiments which have been done on the sample test data.

Based on the information in Tables 4 and 5, it's noticeable that the RMS errors in estimation errors of component positions using KF with Gauss-Markov modeling in SA on and off modes declined to less than 7.5 and 1.2 meters, respectively.

Figures 10 and 13 demonstrate the real, predicted

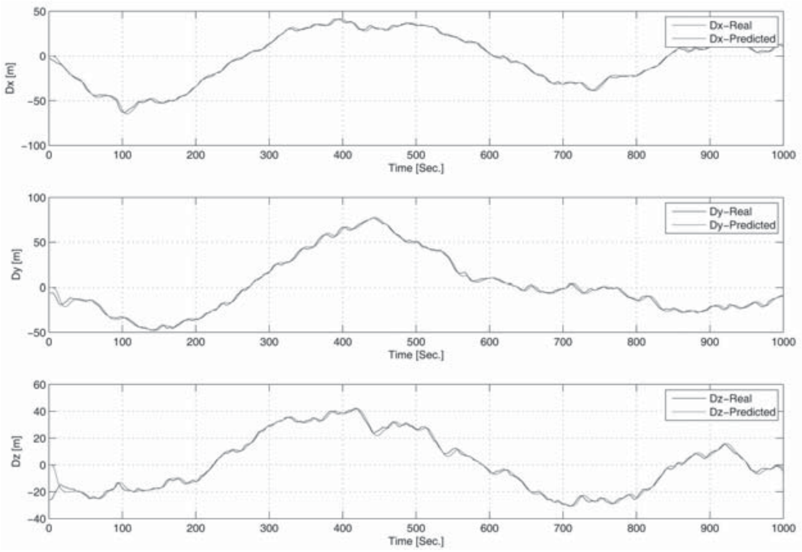


**Figure 6.** The results of 1000 prediction for component positions using KF with Gauss-Markov modeling (SA on).

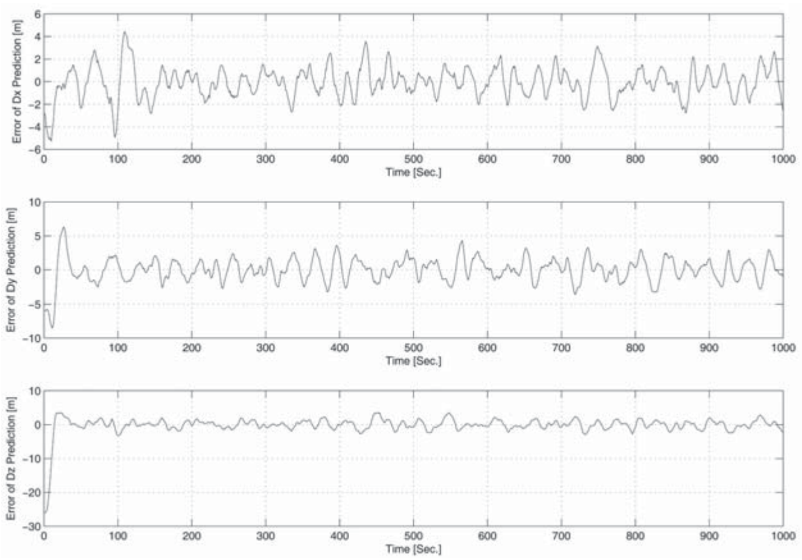


**Figure 7.** The results of 1000 prediction error for component positions using KF with Gauss-Markov modeling (SA on).

and prediction error values of the component position errors for 1000 experimental data sets using KF with variable transition matrix in SA error turned on and turned off modes.

**Table 4.** Minimum, maximum, average, and RMS of errors in predicting 1000 experimental data sets using KF with Gauss-Markov matrix (SA on).

| Parameters | x | y | z |
|---|---|---|---|
| Max | 4.4338 | 6.3375 | 3.5531 |
| Min | -5.2681 | -8.5273 | -26.0181 |
| Average | 0.0511 | 0.0171 | 0.1626 |
| RMS | 1.9333 | 3.1685 | 6.4422 |
| **Total RMS** | **7.4350** | | |

Tables 6 and 7 include the statistical features of experiments which have been done on test data.

According to the information in Tables 6 and 7, the RMS errors in estimation errors of component

**Table 5.** Minimum, maximum, average, and RMS of errors in predicting 1000 experimental data sets using KF with Gauss-Markov modeling (SA off).

| Parameters | x | y | z |
|---|---|---|---|
| Max | 2.4061 | 3.0893 | 2.5399 |
| Min | -3.1232 | -2.6064 | -2.1410 |
| Average | 0.0106 | -0.0215 | 0.0011 |
| RMS | 0.8006 | 0.6234 | 0.5005 |
| **Total RMS** | **1.1314** | | |

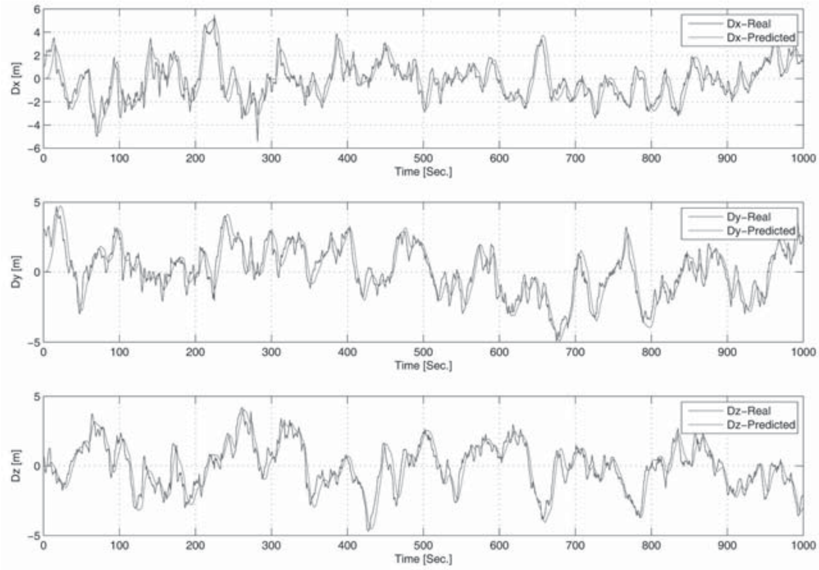


**Figure 8.** The results of 1000 prediction for component positions using KF with Gauss-Markov modeling (SA off).

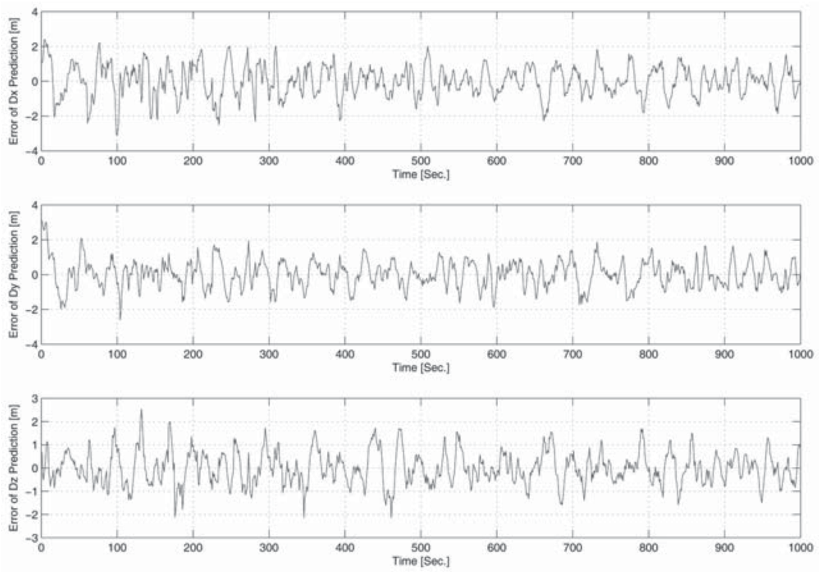


**Figure 9.** The results of 1000 prediction error for component positions using KF with Gauss-Markov modeling (SA off).

positions using KF with variable transition matrix in SA on and off modes decreased to less than 1 and 0.9 meters, respectively.

**Table 6.** Minimum, maximum, average, and RMS of errors in predicting 1000 experimental data sets using KF with variable transition matrix (SA on).

| Parameters | x | y | z |
|---|---|---|---|
| Max | 1.2327 | 1.6291 | 1.4203 |
| Min | -2.5791 | -1.9614 | -1.5044 |
| Average | 0.0181 | -0.0049 | 0.0204 |
| RMS | 0.5627 | 0.6123 | 0.4987 |
| **Total RMS** | **0.9697** | | |

**Table 7.** Minimum, maximum, average, and RMS of errors in predicting 1000 experimental data sets using KF with variable transition matrix (SA off).

| Parameters | x | y | z |
|---|---|---|---|
| Max | 2.7573 | 2.1463 | 1.8208 |
| Min | -2.5797 | -2.2583 | -2.6263 |
| Average | -0.0008 | 0.0040 | -0.0057 |
| RMS | 0.5467 | 0.4607 | 0.4290 |
| **Total RMS** | **0.8338** | | |

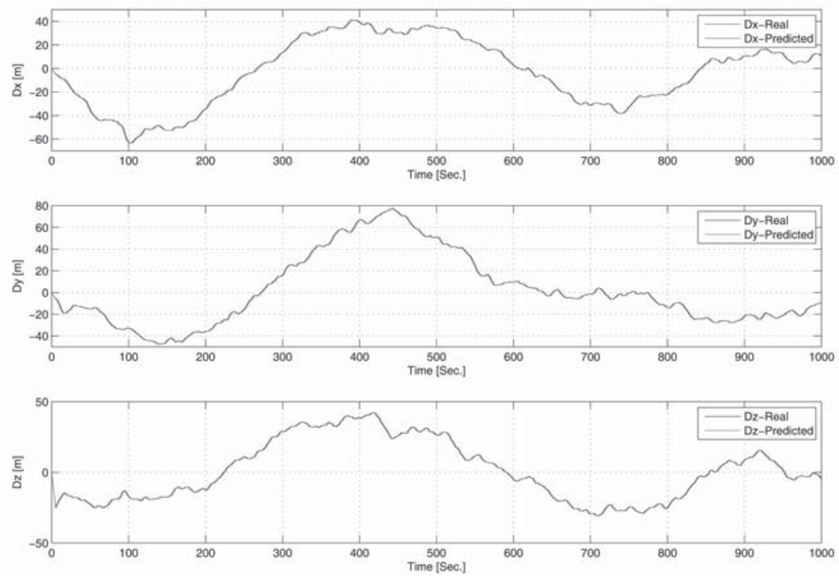


**Figure 10.** The results of 1000 prediction for component positions using KF with variable transition matrix (SA on).

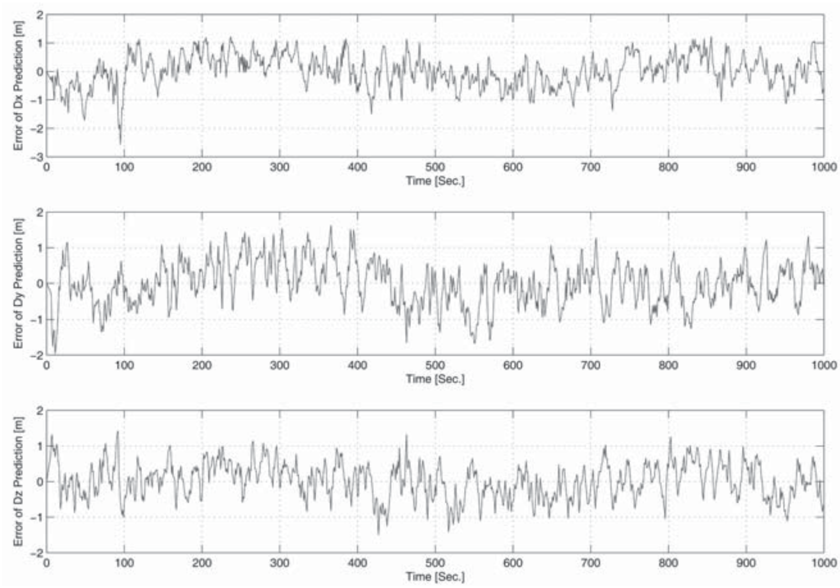


**Figure 11.** The results of 1000 prediction error for component positions using KF with variable transition matrix (SA on).

Table 8 shows the comparing DGPS corrections prediction accuracy using three proposed methods.

**Table 8.** Comparing DGPS corrections prediction accuracy using three proposed methods.

| Prediction Method | Accuracy (SA on) | Accuracy (SA off) |
|---|---|---|
| KF with constant transition matrix | 1.4380 | 0.8108 |
| KF with Gauss-Markov modeling | 7.4350 | 1.1314 |
| KF with variable transition matrix | 0.9697 | 0.8338 |

As shown in Tables 2 to 7, the KF with variable transition matrix has better accuracy than other methods for DGPS corrections prediction.

There are few papers that predict the DGPS corrections using KF. The proposed KFs in this paper have more accuracy than them.

## CONCLUSION

Since GPS is increasingly used worldwide and it has become an essential part of different fields of commerce and military, subjects such as improvement in measurement accuracy and data security in GPS systems are

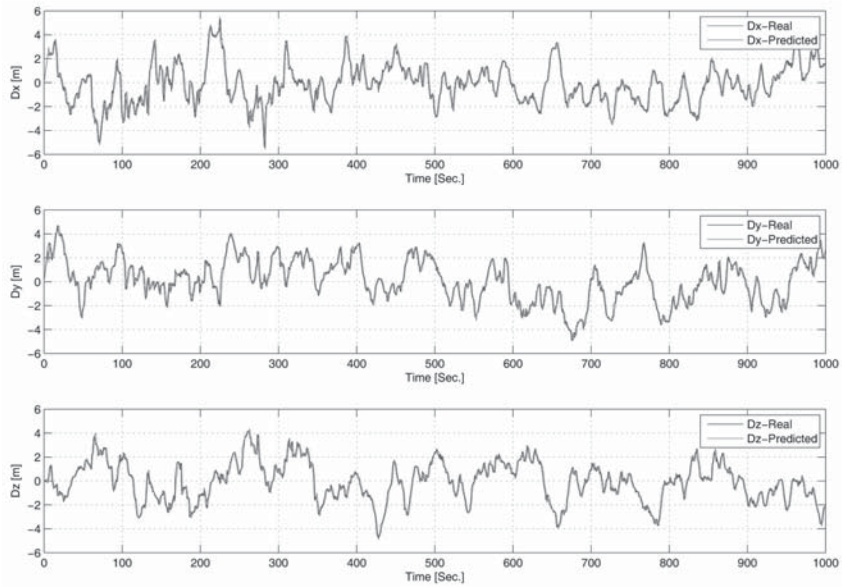


**Figure 12.** The results of 1000 prediction for component positions using KF with variable transition matrix (SA off).

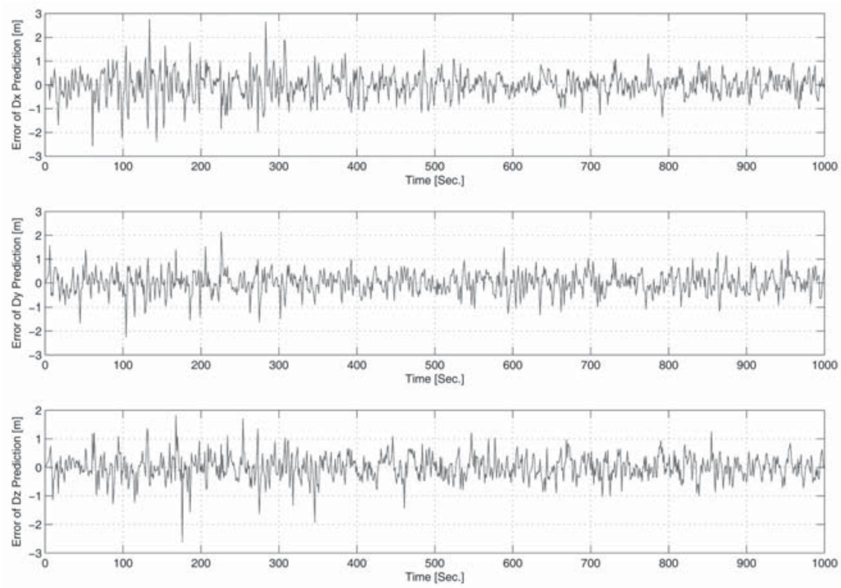


**Figure 13.** The results of 1000 prediction error for component positions using KF with variable transition matrix (SA off).

not only theoretical issues but also vital requirements in these systems. In this paper, the way of utilizing an inexpensive GPS receiver as a precise positioning device as well as algorithms based on KF with the purpose of estimating DGPS corrections were suggested. The experimental results on real data which collected in test fields, gaurantee the high potential of these methods to gain accurate positioning information. The results demonstrated that it is possible to reduce position RMS errors in single-frequency GPS receivers to less than one meter.

## REFERENCES

1. Parkinson B.W., Spilker Jr J.J., Axelrad P. and Enge P., "Global Positioning System: Theory and Applications", *The American Institute of Aeronautics and Astronautics*, (1996).

2. Mosavi M.R., "A Practical Approach for Accurate Positioning with L1 GPS Receivers using Neural Networks", *Journal of Intelligent and Fuzzy Systems*, **17**(2), PP 159-171(2006).

3. Wu S.C. and Melbourne W.G., "An Optimal GPS Data Processing Technique for Precise Positioning", *IEEE Transactions on Geosciences and Remote Sens-*

*ing*, **31(**1**)**, PP 146-152(1993).

4. McDonald K.D., "The Modernization of GPS: Plans, New Capabilities and the Future Relationship to Galileo", *Journal of Global Positioning System*, **1(**1**)**, PP 1-17(2002).
5. Qvstedal O., "Absolute Positioning with Single-Frequency GPS Receivers", *Journal of GPS Solutions*, **5(**4**)**, PP 33-44(2002).
6. Dyke K.L.V., "The World after SA: Benefits to GPS Integrity", *IEEE Conference on Position, Location, and Navigation*, PP 387-394(2000).
7. Mosavi M.R., "Precise Real-Time Positioning with a Low Cost GPS Engine using Neural Networks", *Journal of Survey Review*, **39(**306**)**, PP 316-327(2007).
8. Tsai Y.J., "Wide Area Differential Operation of the Global Positioning System: Ephemeris and Clock Algorithms", Ph.D. Thesis, Stanford University, (1999).
9. Simon D., *Optimal State Estimation Kalman,* $H_\infty$*, and Nonlinear Approaches*, John Wiley, (2006).
10. Farrokhi H., Mosavi M.R., and Nakhaei A., "Prediction of DGPS Corrections using Kalman Filter", *The 30th Asian Conference on Remote Sensing (ACRS 2009)*, China, (2009).
11. Mosavi M.R., "Infrared Counter-Countermeasure Efficient Techniques using Neural Network, Fuzzy System, and Kalman Filter", *Iranian Journal of Electrical and Electronic Engineering*, **5(**4**)**, PP 215-222(2009).
12. Papoulis A. and Pillai S.U., *Probability, Random Variables and Stochastic Processes*, 4rd Edition, McGraw-Hill, (2002).
13. Mosavi M.R., Mohammadi K., and Refan M.H., "Time varying ARMA Processing on GPS Data to Improve Positioning Accuracy", *The Asian GPS Conference 2002*, PP 125-128(2002).
14. Rockwell Semiconductor Systems, "Zodiac GPS Receiver Family Designer[s Guide", (1996).